Proceedings of the 14th European Wave and Tidal Energy Conference 5-9th Sept 2021, Plymouth, UK
Pages 2182-1-2182-9
September 2021,

https://archimer.ifremer.fr/doc/00736/84812/

ResourceCODE framework: A high-resolution wave parameter dataset for the European Shelf and analysis toolbox

Accensi Mickael [1], Alday Gonzalez Matias Felipe [5], Maisondieu Christophe [2], Raillard Nicolas [2], Darbynian David [6], Old Chris [9], Sellar Brian [9], Thilleul Olivia [3], Perignon Yves [3], Payne Gregory [3], O'Boyle Louise [8], Fernandez Leandro [7], Dias Frederic [7], Chumbinho Rogerio [8], Guitton Gilles [4]

[1] IFREMER, LOPS, Plouzané, France
[2] IFREMER, LCSM, Plouzané, France
[3] Ecole Centrale Nantes, Nantes, France
[4] OceanDataLab, Plouzané, France
[5] CNRS, LOPS, Plouzané, France
[6] EMEC, Orkney, UK
[7] University of Dublin, Dublin, Ireland
[8] WiseBlue Marine, Galway, Ireland
[9] University of Edinburg, Edinburg, UK

Abstract :

Resource mapping is a key element in the planning and consequent deployment of Offshore Renewable Energy (ORE) converters. A proper characterization of the environmental forcing enables the optimization of energy extraction and a more accurate assessment of the structural loading. This contributes to improving reliability and extending the operational life of devices at a given extraction site. Providing an accurate characterisation of the environmental loading is subjected to the availability and quality of relevant datasets, which are either obtained from measurements, in-situ or via remote sensing, or from numerical models. Then, the adequate use of these datasets relies on the analysis' tools and selected methods which allow an appropriate description of the underlying physics. This paper presents the high-resolution wave hindcast database extending across European waters and developed to be the reference dataset of the ResourceCODE Marine Data Toolbox, designed to provide a full suite of tools to support ocean energy analytics.

Keywords : Hindcast database, Statistics, Analytical tools.

I. INTRODUCTION

Resource mapping is essential for the optimal planning of the deployment of Offshore Renewable Energy (ORE) converters. A proper characterization of the environmental forcing enables optimization of energy extraction and a more accurate assessment of the structural loading, hence contributing to ensuring reliability and extending the operational life of devices at a given production site.

Providing an adequate characterisation of the environmental loading requires availability of relevant datasets, either obtained from measurement, in-situ or remote, or from modelling as well as the suitable data analysis tools and procedures allowing for a better description of the underlying physics.

The objective of ResourceCODE is to provide a full suite of tools to support ocean energy analytics, elaborated to underpin design and operational decisions for ORE deployments. The ResourceCODE tool suite is supported by a comprehensive hindcast database of high-resolution ocean energy resource parameters for European waters.

The configuration of the ResourceCODE wave hindcast model is based on a high-resolution unstructured grid extending from the south of Spain to the Faroe Islands and from the western Irish continental shelf to the Baltic Sea. Forcing winds are extracted from the ERA5 database while the currents and water levels are recomposed from a database of harmonics of tidal currents (MARS and FES2014).

These forcing fields have been used to run WAVEWATCH-III® to generate a 28-year metocean database covering the [1993-2020] period with an hourly time step. A set of 39 global parameters as well as the frequency spectra are made available as output at each of the 328 000 nodes of the grid while directional spectra are provided on a coarser grid.

The model configuration and dataset have been extensively validated against measurement data, both in-situ and remote. Special consideration was given to the assessment of the spectral distribution of the energy within sea-states spectra.

In addition to the basic time series descriptive statistics, the ResourceCODE Marine Data Toolbox provides developers with a set of standard functions for resource assessment and operations planning, including a capability for comparison with collocated in-situ measurement datasets. The advanced statistical modelling tools provided allows the developers to conduct the necessary assessments to reduce uncertainty in expected environmental conditions, and de-risk investment in future technology design.

The open source services offered in the ResourceCODE Marine Data Toolbox will be accessed through an online platform, specifically designed to facilitate the use of its different applications - test facilities, the supply chain and renewable technologies developers undertaking pre-commercial demonstration (TRL4 to TRL 8) -, data access and processing, as well as output visualisation and storage.

The ResourceCODE Marine Data Toolbox will provide reliable, traceable, and validated data to support the ORE industry by contributing to reducing design and development cost.

II. THE RESOURCECODE WAVE HINDCAST DATABASE

The wave hindcast database is a major feature of the ResourceCODE Marine Data Toolbox. It was built running the WAVEWATCH-III® (WW3) model using a specifically designed configuration, aimed to take into account a wide variety of geographic, bathymetric and bottom type features within Europe. From deep open water conditions of the North Atlantic at the western boundary, to intricate coastlines and archipelagos at Northern Scotland, to strong tide influenced regions like the English Channel (Fig.1 and Fig.2). This results in very different hydrodynamic scenarios affecting wave generation (different fetch limitations), propagation (i.e. current induced refraction) and dissipation (i.e. bottom friction).

Given the different environmental conditions, quality control and validation is of special importance to ensure the reliability of the provided wave parameters. Therefore, different approaches have been utilized to assess the hincast results, based on comparison with remote sensing and in situ buoy data.

A. Wave model configuration

The hindcast was generated using the latest version of the WW3 phase-averaged model [31]. The model was run using the latest parameterization tuning from test T475 [1], which includes adjusted parameters for the wind-wave generation and swell dumping terms, and an extended spectral frequency range.

The model configuration is based on a high-resolution unstructured grid, which nodes' spatial distribution is mainly constrained using time step restrictions obtained from an explicit propagation scheme. Criteria for specific refinement considered the propagation velocity and the bathymetry gradients, allowing for the optimisation of the computational time by limiting the minimal size of the smallest triangle elements. Overall, using this type of mesh facilitates solving intricate or abrupt bathymetric changes and high current gradients over a reduced geographic space [26] [27]. These features are commonly observed in coastal areas [28] [8] [13]. The mesh thus provides an adaptive spatial resolution that makes solving wave-current interactions more efficient than a complex grid nesting scheme.

The resolution within the modelled domain evolves from about 10 km offshore to about 200 m in shallow coastal areas. The unstructured grid is composed of over 328000 nodes and extends from the south of Spain to the Faroe Islands, and from the western Irish continental shelf to the Baltic Sea [-12°W to 13.5°E, 36°N to 63°N].

1) Parameterization and spectral discretization

The parameterization for wave generation is taken from [18] with later modifications by Bidlot et al. [6] [7]. Swell damping effects due to air-sea interactions are those of [4], with the adjustments and modifications detailed in [5] and [20]. Coastal reflection effects are introduced with a constant ad-hoc coefficient using the parameterization proposed by [2].

Wave dissipation induced by the seabed roughness is based on the ripple roughness predictor [15] for sandy bottom, adapted for irregular waves and so as to take into account the variability of the nature of the seabed. Hence, a mapping of the seabed was implemented, based on the grain size classification defined in the EMODnet Geology Seabed substrate database (EMODnet 2016).

Directional spectra computed at each time step and at each node of the grid are discretized over 36 directions of 10° bins and 36 exponentially spaced frequencies from 0.0339 Hz to 0.9526 Hz.

The full list of parameters' values is presented in Appendix A.

2) Numerical choices and time step selection

The wave action equation (WAE) is solved using a splitting method to treat temporal depth changes, spatial propagation, intra-spectral propagation and source terms in different steps. Wave action propagation is done with the ULTIMATE-QUICKEST explicit third order scheme [21], while nonlinear evolution and wave to wave interactions are represented with the discrete interaction approximation [17].

For the present configuration of WW3, a good balance between the required cpu time and the accuracy of the simulated wave fields was obtained with the following time steps: Max. overall time step = 180 s, max. advection time step = 30 s, max. refraction time step = 15 s, and an overall min. time step = 5 s.

The 28-year hindcast generation took approximately 2,000,000 cpu hours distributed over 18 nodes. Where each node is composed of 28 CPUs and 60Gb of memory.

3) Bathymetry

An accurate mapping of the bathymetry is necessary, especially in coastal areas and over the extension of the continental shelf, to properly account for refraction phenomena. The bathymetry within the domain is taken from the EMODnet dataset (EMODnet 2016), combined with the HOMONIM dataset provided by SHOM (MNT 0.001° resolution) which covers the Channel and the Bay of Biscay. Both data sources' vertical datum is defined with respect to the mid sea level (MSL). After integrating the gridded datasets, the final array was interpolated into the nodes of the computational grid.

4) Wind Field

Forcing wind fields are taken from the fifth generation ECMWF atmospheric reanalyses of the global atmosphere, ERA5 [17]. The ERA5 winds present hourly output with a 31 km horizontal grid resolution. This is a clear improvement in the fields' detail compared to its predecessors like ERA-Interim [11].

As detailed in [1], the use of the ERA5 wind fields for the hindcast generation required a thorough parameters' tuning. This process was focused first on the definition of an adequate wind-wave growth parameter (β_{max}) to reduce overall biases due to wind strength, as done in [30]. And then, adjustments of the dissipation parameterization terms (s7 and Re_c) proposed in [4], which helped to improve the wave height distributions at global and local scales.

Within this process, a bias correction for high winds was applied to enhance the ERA5 intensities larger than 21 m/s. The defined threshold to apply the wind correction, aligns with the analysis performed by [25], where it was found that ECMWF models typically underestimate intensities above 20 m/s (compared to in-situ data).

The final parameters used are the same as those proposed in test T475.

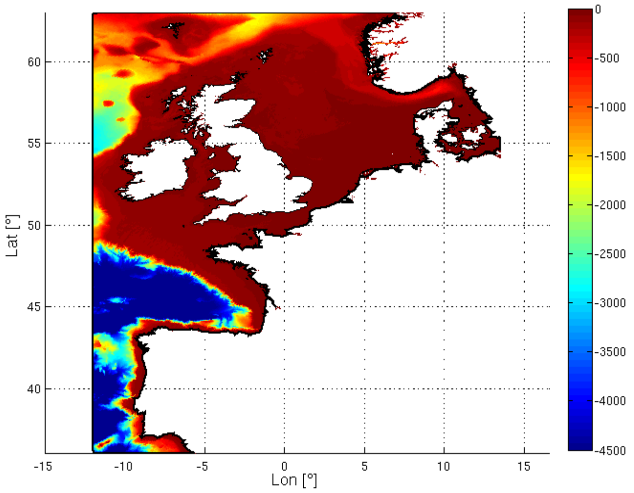

Fig. 1. Integrated bathymetry interpolated into the ResourceCODE mesh nodes. Colorbar shows depth values in meters w/r to MSL. Black lines are the boundary and land polygons.

5) Currents and water levels

Currents and water levels have a strong influence on the evolution of sea-states, especially in coastal areas having shallower depths and where tidal currents of higher intensity may affect wave trains propagation [2].

The evolution in time of current intensities and directions as well as sea water levels, are reconstructed at each node of the modelled domain using tidal harmonics. To cover the complete region of the model, two different sources of harmonics were employed: from MARS 2D [19], and the FES2014 database.

MARS 2D is a hydrodynamic model based on the shallow water equations [19]. Tidal harmonics from this model are taken from the Tidal Atlas developed and validated at Ifremer [24]. A total of 5 models with 3 levels of nesting, and spatial resolution were selected. The lowest nesting level 0 corresponds to the largest modelled domain where all the other sub-models are nested. The details of the selected models from Ifremer's tidal atlas is presented in Fig. 2.

The second tidal data source was used to cover part of the Atlantic coast from Portugal to the northern end of the Gibraltar strait (which are not included in Ifremer's tidal atlas). This data was taken from the native mesh of the FES2014 model [9], and re-gridded to 0.004° (~450 m) before its use.

The generated forcing fields are updated with a 30 mn time step in WW3.

It should be noted that even though their quality is deemed good enough for the evaluation of the wave-current interaction and wave refraction, such recomposed current fields and water levels might be less accurate than those directly obtained from high resolution hydrodynamic models, especially in some shallow areas or intricate archipelagos, where caution is advised when performing a tidal resource assessment.

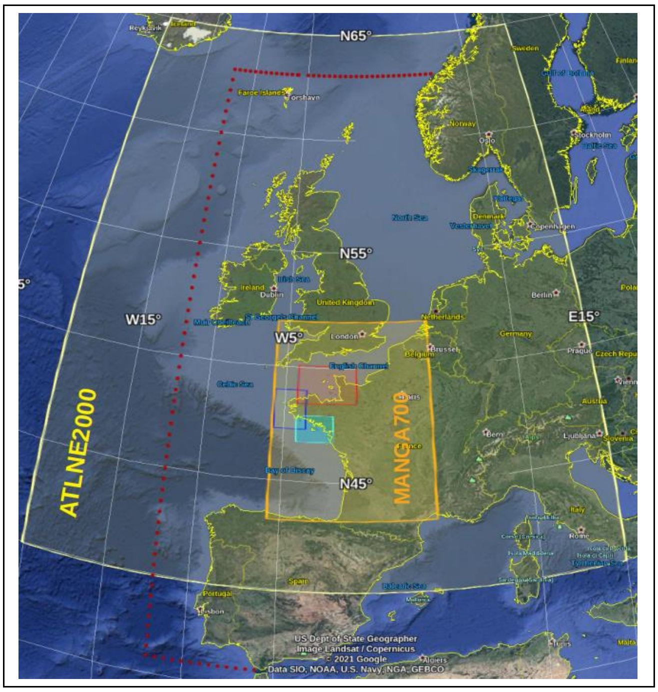

Fig. 2. Nested models from Tidal Atlas. Blue rectangle shows the area of FINIS250 model, Light blue rectangle shows the area of SUDBZH250, and Red rectangle shows the area of MANW250. Red circles show the nodes along the model open boundary where spectral conditions are prescribed.

TABLE I
NESTED CURRENT MODELS EXTENSION AND REFERENCES

Nesting Level	Spatial resolution [m]	Model domain limits		Region	Model Name
		Longitude [°]	Latitude [°]		
0	2000	-20.03 to 14.98	39.98 to 64.98	North-East Atlantic	ATLNE 2000
1	700	-5.73 to 4.18	43.28 to 52.00	Channel & Bay of Biscay	MANGA 700
2	250	-5.63 to -3.66	47.34 to 49.03	Iroise Sea	FINIS250
2	250	-4.23 to -1.96	46.78 to 47.93	South Brittany	SUDBZH 250
2	250	-4.21 to -0.50	48.45 to 50.10	Western channel	MANW 250

6) Open Boundaries directional spectra

Wave directional spectra used as input along the open boundaries (Fig.2) are extracted from a global database built running WW3 on a 0.5° regular grid. The spectral discretization of the global grid covers the same range and number of frequencies as used in the ResourceCODE mesh, and 24 directions (directional resolution of 15°). Parameterization settings are those of test T475.

Forcing fields used in the global model are: ERA5 wind fields, CMEMS-Globcurrent surface current fields (Global Ocean Multi Observation Product, MULTIOBS_GLO_PHY_REP_015_004), ice concentration distribution from the Ifremer SSMI-derived daily product [14] and the Ifremer-Altiberg icebergs distribution database [1] to take into account partial wave blocking [3].

The spectral boundary conditions (BC) are defined at 104 nodes along the open boundary (Fig.2), which are then spatially interpolated at the remaining boundary nodes. The global model provides output each 3 hours, which implies a temporal interpolation of the BC to update the spectra input every hour. Finally, to match the directional discretization used in the ResourceCODE mesh, a directional interpolation is applied to the BC spectra.

B. Wave model output

With the objective of ResourceCODE to provide relevant information and adapted analysis tools for the design and optimisation of ORE devices, considering both resource assessment and environmental loading, it is important that the data provided as output of the hindcast model be comprehensive and adapted to the needs and requirements of the users. Hence, three different output datasets were produced, namely global parameters, frequency spectra and directional spectra.

1) Global parameters

An ensemble of 39 global parameters is made available as output at each node of the computational grid and at each time step. These include the forcing fields (wind and current intensities and directions), the standard mean wave parameters such as the significant wave height, the peak period or the wave peak and mean directions but also parameters of relevance for ORE such as the energy flux CgE, the energy period Te or the directional spreading. They also include the standard parameters associated with the wave systems composing the sea-states and obtained after spectral partitioning [31].

Additional parameters are also made available, of relevance for sediment transport, such as orbital amplitude and velocity near the seabed or for ocean-atmosphere interactions, such as friction velocity, stokes drift, wave to wind stress and wave to ocean stress. The full list of output parameters is given in APPENDIX B.

2) Frequency spectra

Frequency spectra are widely used for the assessment of the response of ORE devices, especially omnidirectional systems, considering various dynamic or structural degrees of freedom and under linear systems assumption. Hence 36 components frequency spectra are saved at each node of the computational grid and at each time step.

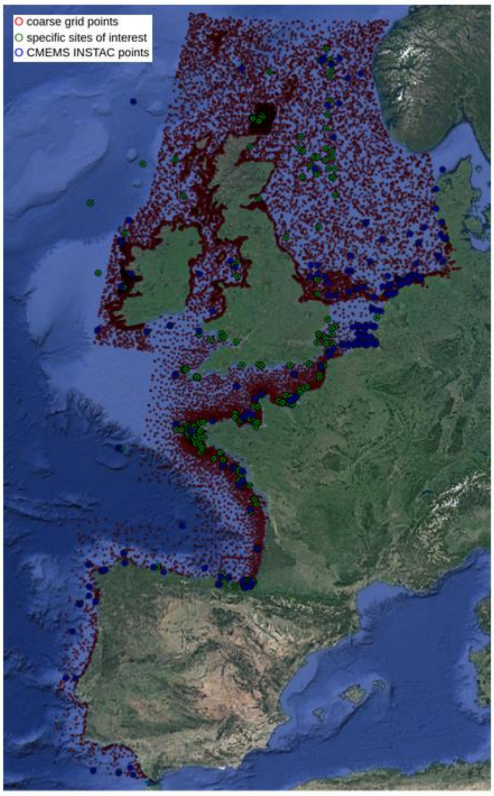

Fig. 3. Directional spectra output locations

3) Directional spectra

Directional spectra provide the most comprehensive information on the wave energy distribution within sea-states, especially when considering multimodal wave conditions. Because of some limitations in the data handling and storage capacity, saving directional spectra at each node of the grid and on an hourly basis was simply not possible. However, in order to provide the most relevant dataset and considering the objectives of the ResourceCODE Marine Data Toolbox, a coarser output grid was created, derived from the computational grid, on which these directional spectra are saved at each time step. This grid also includes a series of additional nodes corresponding to specific sites of interest for the ORE community such as testing sites (EMEC, SEMREV, AMETS, SmartBay, Westwave,…) or sites already identified as being of potential interest for production, (wave, offshore wind). Sites corresponding to *in-situ* stations used for validation of the model were also added to this list (Fig.3). Altogether a set of 24162 directional spectra (36 directions x 36 frequencies) were saved at each time step.

C. Wave Model Validation

To fully assess the model performance, an extensive validation work was conducted based on the derivation of statistical error estimators established comparing the model data with wave buoys and remote sensing data. Reference parameter used for this validation was mainly the significant wave height. However, spectral validation over frequencies following the methodology presented in [22] and applied a posteriori for the analysis of HOMERE in [23] was also conducted at locations where wave spectra derived from wave buoys were available.

The normalized bias (NB), normalized root mean square difference (NRMSE), scatter index (SI) and correlation coefficient (R) are employed as performance estimators.

$$NB(X) = \frac{\sum(Xmod - Xobs)}{\sum Xobs}$$

$$NRMSE(X) = \sqrt{\frac{\sum (Xmod - Xobs)^2}{\sum Xobs^2}}$$

$$SI(X) = \sqrt{\frac{\sum[(Xmod - \overline{Xmod}) - (Xobs - \overline{Xobs})]^2}{\sum Xobs^2}}$$

$$R(X) = \frac{\sum(Xmod - \overline{Xmod})(Xobs - \overline{Xobs})}{\sqrt{\sum (Xmod - \overline{Xmod})^2 \sum (Xobs - \overline{Xobs})^2}}$$

With X for any quantity of modeled data (Xmod) and observation data (Xobs). The overbar denotes the arithmetic average.

1. Altimeter Data

The sea surface wave height estimated by the altimeter database from the CCI Sea State V1 [12] for the period 1994-2018 was used. It offers a good consistency in space and time to assess the overall model performance. The study area is covered by all the altimeters provided except Cryosat-2 which is in SAR mode in the North-East Atlantic. Due to issues on the onboard instrumentations, ERS-1 data after 1995 and ERS-2 data after 2002 were not used. Data from currently working satellites Saral and Jason-2 were not yet available for 2019 and 2020 in this version.

The methodology applied for this model validation was to obtain matches-up of the model output along each altimeter track by performing a spatio-temporal interpolation. Altimeters data considered unreliable (tracks within 50km from coasts, significant wave height lesser than 1m and affected by noise) were disregarded. A merged product is then generated by gathering all the altimeters data available to produce the following yearly analysis.

Overall statistics presented in table II indicate a good agreement between model and altimeter data for all altimeters which allow us to assess the overall model performances for the significant wave height with really encouraging scores on the merged satellite product from 1994 to 2018. The normalised bias is 0.26% (0.7cm) with a NRMSE at 10.30% (30.7cm). The scatter index is very similar to the NRMSE which shows a limited impact of the bias on the random error. The correlation coefficient is steady around 97%.

TABLE II
OVERALL STATISTICS PER ALTIMETER

Satellite	Covered period	B (m)	NB (%)	RMSE (m)	NRMSE (%)	SI (%)	R (%)
ERS-1	1994-1995	0.021	1.20	0.300	10.61	9.05	93.87
TOPEX	1994-2005	-0.013	-0.32	0.325	10.52	10.16	97.11
ERS-2	1995-2002	0.004	0.23	0.308	10.73	10.03	96.08
GFO	2000-2008	0.008	0.44	0.315	10.37	9.85	96.96
JASON-1	2002-2013	0.001	0.04	0.307	10.06	9.56	96.90
ENVISAT	2002-2012	0.011	0.47	0.292	9.86	9.06	96.11
JASON-2	2008-2018	0.011	0.28	0.308	10.08	9.56	96.92
SARAL	2013-2018	0.015	0.47	0.279	9.42	8.64	97.03
JASON-3	2016-2018	0.014	0.37	0.292	10.14	9.78	97.16
MERGED	1994-2018	0.007	0.26	0.307	10.30	9.82	96.80

The time series of the statistical estimators (Fig.4) reveal a good correlation over years with a trend to better scores and lower fluctuations in recent years. The important point is to demonstrate that model performances are steady over the covered period with less than 2% of variation for the SI, NRMSE and NB.

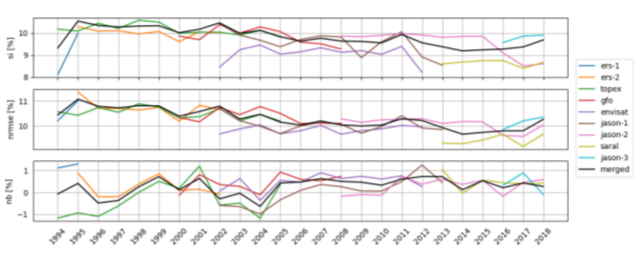

Fig. 4. Overall time series of SI, NRMSE and NB

The along-track data were averaged over a regular 1/8° grid to allow further yearly estimates (Fig. 5).

The benefit of the altimeter global coverage is to supply a map of significant wave height with a sufficient amount of yearly matches-up (Fig. 5c) to compute confident estimates (Fig. 5d) on the whole domain. The NB (Fig. 5a) and NRMSE (Fig. 5b) reveal some interesting patterns to further investigate. The Scottish Sea has a positive bias associated with a higher random error. The South-West of the North Sea has a lower correlation coefficient related to a negative bias and a stronger RMSE. On average, NB tends to be positive in the Atlantic Ocean and negative in the North Sea. The NRMSE and NB increase in shallow water and sheltered areas.

Those discrepancies can be due to both altimeters' errors, model parameterization and wind and current forcing fields.

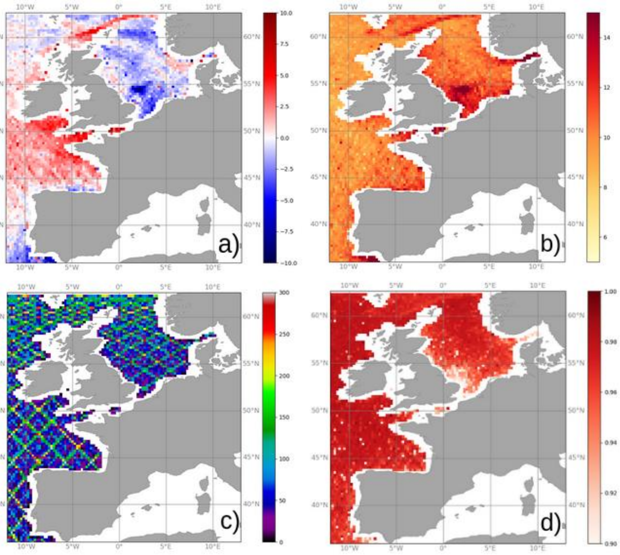

Fig. 5. yearly estimates averaged over 1993-2018. a) NB; b) NRMSE; c) matches-up; d) R

2. In-situ data

The *in-situ* validation dataset is composed of two types of data:

- Global integral parameters from In SituTAC database [5]
- Frequency spectra provided by national research centres at various locations along coasts (Cerema and Centrale Nantes in France, Marine Institute Ireland, EMEC in Scotland, Cefas Wavenet in the UK)

The validation on integral parameters is performed on selected locations across the EU: EMEC (BC), AMETS, SEM-REV, PIERRES NOIRES, and SmartBay. Integral parameters are H_{m0}, T_p, θ_p, and θ_s. The buoy data are archived using the Copernicus InsituTAC data standard. The standardised variable names are used to select validation parameters from the buoy records; the corresponding buoy parameter names are VHM0, VTPK, VPED, VPSP. Not all buoys have all of these parameters, so the coverage varies by parameter.

The validation of integrated parameters is applied on a month-by-month basis. Buoy data are cleaned using the relevant parameter QC flags (data samples not meeting the criteria are rejected). The remaining data are mapped onto the model's hourly timestamps using a nearest neighbor mapping with a minimum time difference threshold of ±1.5 hours. If fewer than 50% of the model timestamps are matched to buoy data then the buoy record is rejected, otherwise the validation parameters are calculated using the data flagged as "good" and the results tabulated.

Results on NB, NRMSE, SI and R are presented in the tables below. Data from the five sites were processed for the years 2015 to 2019 inclusive. The average values over all months at each site for each validation parameter are presented in the Table III.

TABLE III
PARAMETER STATISTICS PER SITE (2015-2109)

(a) Significant Wave Height (H_{m0})

Site	B [m]	NB [%]	RMS [m]	NRMS [%]	SI [%]	R [%]
EMEC (BC)	0.02 (±0.03)	1.1 (±1.5)	0.27 (±0.07)	12.6 (±2.3)	11.1 (±2.3)	96.7 (±2.3)
AMETS	0.004 (± 0.07)	0.6 (±2.7)	0.35 (±0.10)	11.3 (±1.4)	10.2 (±1.1)	95.9 (±1.5)
SEM-REV	0.05 (±0.07)	3.5 (±4.3)	0.25 (±0.07)	13.9 (±2.6)	11.5 (±1.6)	96.2 (±2.0)
PIERRES NOIRES	0.24 (±0.06)	12.5 (±4.7)	0.37 (±0.09)	18.8 (±4.4)	12.3 (±1.6)	95.9 (±1.9)
SMART BAY	-0.20 (±0.05)	24.6 (±3.8)	0.25 (±0.06)	31.8 (±4.4)	17.3 (±2.7)	94.9 (±1.9)

(b) Peak Wave Period (T_p)

Site	B (s)	NB (%)	RMS (s)	NRMS (%)	SI (%)	R (%)
EMEC (BC)	-0.09 (±0.18)	-0.8 (±1.6)	1.5 (±0.2)	14.3 (±2.0)	13.9 (±2.0)	74.0 (±5.2)
AMETS	-0.20 (±0.19)	1.8 (±1.8)	1.28 (±0.24)	11.6 (±2.2)	11.2 (±2.2)	76.3 (±8.2)
SEM-REV	-0.03 (±0.22)	0.2 (±2.1)	1.70 (±0.42)	16.0 (±3.9)	15.5 (±3.7)	71.6 (±12.6)
PIERRES NOIRES	-0.13 (±0.24)	1.2 (±2.2)	1.60 (±0.60)	14.6 (±5.3)	14.1 (±4.7)	70.6 (±11.4)
SMART BAY	1.91 (±0.68)	27.1 (±8.5)	3.72 (±0.87)	52.8 (±9.7)	41.2 (±6.5)	40.9 (±10.5)

(c) Wave Direction (θ_p)

Site	B (°)	NB (%)	RMS (°)	NRMS (%)	SI (%)	R (%)
EMEC (BC)	-8,4 (±2.3)	-	-	-	-	69.0 (±13.2)
AMETS	-11.4 (±4.4)	-	-	-	-	75.1 (±12.7)
SEM-REV	-2.1 (±4.1)	-	-	-	-	60.3 (±16.0)
PIERRES NOIRES	1.4 (±6.2)	-	-	-	-	60.5 (±16.3)
SMART BAY	0.22 (±7.8)	-	-	-	-	52.2 (±22.3)

(d) Wave Spreading (θ_s)

Site	B (°)	NB (%)	RMS (°)	NRMS (%)	SI (%)	R (%)
EMEC (BC)	2.1 (±1.5)	7.4 (±5.1)	9.5 (±2.3)	33.3 (±7.1)	31.3 (±6.4)	39.1 (±9.9)
AMETS	-	-	-	-	-	-
SEM-REV	0.14 (±4.02)	0.6 (±14.3)	12.5 (±3.3)	44.7 (±100.6)	41.3 (±9.7)	24.2 (±17.8)
PIERRES NOIRES	7.5 (±3.4)	31.7 (±14.3)	12.3 (±3.5)	52.1 (±14.7)	39.3 (±8.8)	33.6 (±13.0)
SMART BAY	-	-	-	-	-	-

The sites chosen are all coastal; EMEC (BC) is on the west coast of the Orkneys, AMETS and SmartBay are on the west coast of Ireland, and SEM-REV and PIERRES NOIRES are on the west coast of Brittany. Among these five sites, two were selected as they are relatively demanding for the model configuration. The SmartBay buoy is located in a sheltered area, close to the shore and PIERRES NOIRES is located in an area affected by strong tidal currents. For all sites the significant wave height is accurately predicted with the largest bias occurring at the PIERRES NOIRES and SmartBay sites. The peak wave period is also relatively well predicted (R<80) even though a larger RMS error is observed at the SmartBay site. Assessment of this parameter is however highly sensitive to the frequency discretization of the model and instruments as well as to the wind temporal and spatial resolution used to force the model. Mean period T02, showing less variability, will be investigated in the future. The peak direction shows a limited bias for the sites located in the Bay of Biscay and facing the open ocean as well as for the SmartBay site where the buoy is closer to the shore and sheltered. However, correlation for this latter is poorer. Agreement at AMETS is not as good (B>10°). The directional spreading was only available for the two sites in the Bay of Biscay. The RMS error is of about 12.5° and the correlation is poor. A larger bias is observed at PIERRES NOIRES where the influence of strong tidal currents occurring at that location is to be further investigated. It must be noted that the directional spreading as already been observed as the least well predicted parameter used to define the spectrum. These results are based on parameters integrated across the full wave spectrum, there are indications that integrated parameters based on spectral partitions will produce more consistent results for the wave period and directional data. Work is on-going to generate the statistics for parameters integrated by spectral partition.

The validation of frequency spectra is performed through the comparison of the modelled annual energy as a function of frequency against in-situ data provided by 26 buoys available over the domain: 8 buoys are located along the west coast of France, 3 are located in Irish waters and 15 around the UK, including 4 buoys at EMEC. Results are presented for 3 representative open sea test sites, AMETS, EMEC and SEM-REV. The spectral content can be considered as the sum of independent frequency bands, and the content in each band over time creates independent time series. Thus, the statistical estimators of error can be used at each bandwidth over wave energy spectrum.

Using the wave power per unit width J [W.m^{-1}] defined from the spectral density E and associated group velocity C_g, the spectral quantity for a given frequency f_i and bandwidth $2 \triangle f_i$ is defined as:

$$J(f_i, \Delta f_i) = \int_{f_i-\Delta f_i}^{f_i+\Delta f_i} \rho g C_g(f) E(f) df$$

The wave power per unit width is computed in frequency for buoy and model data. Comparisons between model output and measured quantities for three locations corresponding to ORE test sites are presented on Fig.6 for *J(f)* over the whole duration of the concomitant periods at each location. Error estimators are presented on Fig.7.

At low frequency, below 0.1 Hz, the discrepancies between modeling and measurement are more pronounced, especially at SEM-REV site which is in shallower water (34 m) compared to AMETS and EMEC (respectively 103 and 60 m depth). The maximum error in terms of NRMSE, NBIAS is reached for 0.04 Hz (i.e. wave periods of 25 s) for the deepest sites and 0.05-0.06 Hz (i.e. wave periods between 16 and 20 s) at SEM-REV.

This seems to indicate that the complex processes at stake at those intermediate to shallow depths such as refraction, dissipation by bottom friction, non-linear transfers or interaction with coastal flows remain difficult to accurately describe in the numerical model.

The high frequencies (above 0.1 Hz) are well resolved with NRMSE below 30% at deepest sites and below 40% at SEM-REV. The NBIAS is below 15% at SEM-REV and 5% for the deepest sites.

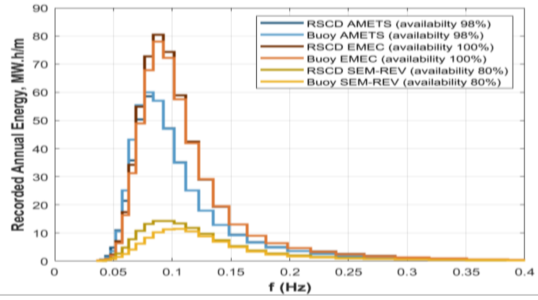

Fig. 6. Mean annual available wave energy in frequency from measurements and RESOURCECODE at three EU test sites locations in 2017

Finally, the spectral error on the annual energy shows that the model is underestimating the measurements at AMETS by 3.7%, overestimating by 4.2% at EMEC and 22.8% at SEM-REV.

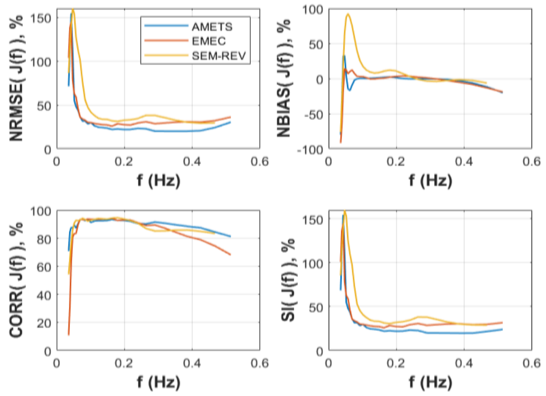

Fig. 7. NRMSE, NBIAS, CORR and SI of the spectral power resource between measurements and RESOURCECODE in 2017.

III. THE RESOURCECODE TOOLBOX

An important objective of the ResourceCODE project, in addition to the implementation of reference datasets, is to provide the tools that will facilitate for users access to the data and allow for the necessary statistical analysis required to contribute to reducing uncertainty in expected environmental conditions, and de-risking investment in future technology design.

Hence an online platform was designed to access the open source services offered by the ResourceCODE Marine Data Toolbox, including efficient data extraction, basic time series descriptive statistics, and advanced statistical modelling tools. Functionality of the toolbox was defined taking into account industry needs assessed through a market research questionnaire.

A. *Web portal for data access*

Because of the spatial extension and high resolution of the model configuration as well as the number of output parameters, the volume of data produced is rather large (about 50 To altogether) and specific tools are needed to facilitate easy and fast access to the data.

Assessment of the end-user's requirements showed that for studies on resource assessment, the design of ORE devices and the planning of Operation and Maintenance (O&M), time series of sea-states parameters are more in demand than mapped data.

Hence, the ResourceCODE web portal is more specifically designed to facilitate the extraction of such time series at a given location. A high-performance unstructured time series database is built to store and access the data (based on Apache Cassandra). This specific structure allows extraction of time series of sea-state parameters as well as the 1D and directional spectra at any node of the computational grid, within a few seconds, for the whole simulated duration or for a selected period of time.

Once data is extracted the user interface implemented on the web portal allows easy handling of data through different services including statistical analysis and plotting of results facilitating control and interpretation of results. All the provided analytical tools are gathered into a standalone python toolbox, that is described in the following section.

B. *Statistical analysis toolbox*

The objective of the ResourceCODE Marine Data Toolbox is to provide ORE developers with a real capacity to conduct the necessary assessments to reduce uncertainty in expected environmental conditions and de-risk investment in future technology design.

Hence, this toolbox provides a set of standard functions for resource assessment, design and operations planning, including a capability for comparison with collocated in-situ measurement datasets.

The various bricks include: comparison with in-situ data, descriptive statistics of any parameter (e.g. seasonality, monthly statistics…); computation of weather windows (both data-based and model based depending on user's inputs); modelling of extreme values (Bloc maxima, Peaks Over Threshold, environmental contours…); producible assessment, based on classical WEC linear transfer functions, with the added possibility to implement user defined transfer functions.

The toolbox is linked to the hindcast database for an easier use, but can also be exploited with any user provided data. It is made available on pypi.org under a LGPL license and is open to contributions for further development beyond the duration of the ResourceCODE project.

C. *In-situ datasets*

In addition to the wave hindcast database, a set of test data will be made available as part of the ResourceCODE Marine Data toolbox for a number of sites around the EU, subject to licensing agreement to be finalized. These datasets however will only include a limited number of parameters and will be of shorter duration compared to the hindcast as they result from various in-situ measurement campaigns.

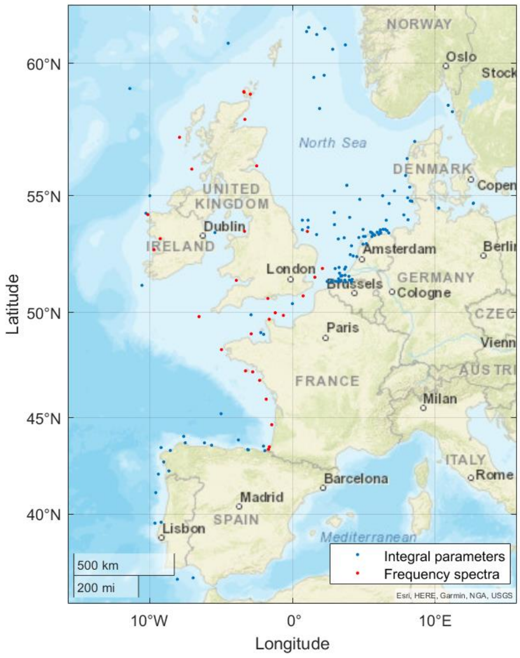

Fig. 7. Map of in situ dataset used for validation of Resource Code using integral parameters and spectral data

Most of these datasets were used for validation purpose. Fig.7 shows a map of in situ datasets composed of both global integral parameters and frequency spectra, as described in section 2. Most of the buoys are Datawell Waverider MkIII instruments recording raw surface displacement at 1.28Hz. The instruments are regularly calibrated and maintained by national oceanographic institutes. The availability of the datasets of omni-directional spectra and wave parameters depends on the buoy location and varies for almost continuous data during several years (except during maintenance periods) to a few months [29] [33].

IV. CONCLUSIONS

The ResourceCODE Marine Data Toolbox presented in this paper aims at providing a full suite of tools to support ocean energy analytics, elaborated to underpin design and operational decisions for ORE deployments, associated with a comprehensive hindcast database of high-resolution ocean energy resource parameters for European waters.

Extensive validation of the dataset against reference in-situ and remote sensing measurement data and including spectral validation methods showed the good quality of the hindcast overall.

The ResourceCODE analysis toolbox provides a set of standard functions for resource assessment, design and operations planning, supported by a web portal specifically designed to facilitate data access and processing.

APPENDIX A - PARAMETERIZATION

The wave model used to produce the hindcast is the version 7 of WAVEWATCH-III (r) with numerical parameterization based on default version 7 of WAVEWATCH-III with the settings T475 from Alday et al. 2021 and some adaptations for unstructured mesh numerical schemes as follows:

1- air-sea interaction parameters (SIN4 namelist)
BETAMAX = 1.75, SWELLF = 0.66, TAUWSHELTER = 0.3, SWELLF3 = 0.022, SWELLF4 = 115000.0, SWELLF7 = 432000.00 /

◎ 2- wave-ice dissipation parameters (SIC2 namelist)

◎ IC2DISPER = F, IC2TURB = 1.0, IC2ROUGH = 0.001, IC2DMAX = 0.3, IC2REYNOLDS = 150000, IC2SMOOTH = 200000., IC2VISC = 2. /

◎ 3- wave-ice scattering (SIS2 namelist)

◎ ISC1 = 0.2, IS2C2 = 0., IS2C3 = 0., IS2BACKSCAT = 1., IS2BREAK = T, IS2DUPDATE = F, IS2CREEPB = 0.2E8, IS2CREEPD = 0.5, IS2CREEPN = 3.0, IS2BREAKE = 1.0, IS2BREAKF = 3.6, IS2WIM1 = 1.0, IS2FLEXSTR = 2.7414E+05, IS2CREEPC = 0.4, IS2ANDISB = T, IS2ANDISD = 0.2E-8, IS2ANDISE = 0.55, IS2ANDISN = 1.0 /

◎ 4- reflexion parameters (REF1 namelist)

◎ REFCOAST = 0.05, REFCOSP_STRAIGHT = 4, REFFREQ = 1., REFICEBERG = 0.2, REFMAP = 0., REFSLOPE = 0., REFSUBGRID = 0.1, REFRMAX = 0.5

◎ 5- other parameters (MISC namelist)

◎ NOSW = 6, WCOR1 = 21., WCOR2 = 1.05

◎ 6- spectral output arrays allocation (OUTS namelist) E3D = 1

◎ 7- unstructured mesh numerical schemes (UNST namelist)

◎ UGBCCFL = F, UGOBCAUTO = T, UGOBCDEPTH = -15.0, EXPFSN = T

◎ 8- Bottom friction (SBT4 namelist)

◎ SEDMAPD50 = T, BOTROUGHMIN = 0.0400, BOTROUGHFAC = 1.0 /

APPENDIX B - OUTPUT PARAMETERS

The model output is given in 8 sections depending on their classification:

1- Forcing Fields
- DPT Water depth.
- CUR Current velocity.
- WND Wind speed.
- WLV Water levels.
- D50 Median sediment grain size.

2- Standard mean wave Parameters
- HS Wave height.
- LM Mean wavelength.
- T02 Mean wave period (Tm0,2).
- T0M1 Mean wave period (Tm0,-1).
- T01 Mean wave period (Tm0,1).
- FP Peak frequency.
- DIR Mean wave direction.
- SPR Mean directional spread.
- DP Peak direction.

3- Spectral Parameters
- EF Wave frequency spectrum
- WN Wavenumber array

4- Spectral Partition Parameters
- PHS Partitioned wave heights.
- PTP Partitioned peak period.
- PLP Partitioned peak wavelength.
- PDIR Partitioned mean direction.
- PSPR Partitioned mean directional spread.
- PWS Partitioned wind sea fraction.
- PDP Peak wave direction of partition.
- TWS Total wind sea fraction.

5- Atmosphere-waves layer
- UST Friction velocity.
- CHA Charnock parameter
- CGE Energy flux
- FAW Air-sea energy flux
- TAW Net wave-supported stress
- TWA Negative part of wave-supported stress
- WCC Whitecap coverage

6- Wave-ocean layer
- TWO Wave to ocean momentum flux
- FOC Wave to ocean energy flux
- TUS Stokes transport
- USS Surface Stokes drift

7- Wave-bottom layer
- ABR Near bottom rms amplitudes.
- UBR Near bottom rms velocities.

8- Spectrum parameters
- MSS Mean square slopes

ACKNOWLEDGEMENT

The ResourceCODE project has received support under the framework of the OCEANERA-NET COFUND project, with funding provided by national/ regional sources and co-funding by the European Union's Horizon 2020 research and innovation programme.

The authors would like to thank Aron Roland and Mathieu Dutour for their support in the mesh generation, Denis Croizé-Fillon for his technical assistance in the HPC computation. The authors also acknowledge contribution of in-situ data from the Marine Institute of Ireland for wave-buoys at AMETS, SmartBay and Westwave.

REFERENCES

[1] Alday, M., Accensi, M., Ardhuin, F., Dodet, G., 2021. "A global wave parameter database for geophysical applications. Part 3: improved forcing and spectral resolution". Ocean Modelling [in press].https://www.essoar.org/doi/abs/10.1002/essoar.10505476.1

[2] Ardhuin, F., and A. Roland, 2012. Coastal wave reflection, directional spread, and seismoacoustic noise sources, J. Geophys. Res., 117, C00J20.

[3] Ardhuin, F., Tournadre, J., Queffelou, P., Girard-Ardhuin, F., 2011. Observation and parameterization of small icebergs: drifting breakwaters in the Southern Ocean. Ocean Modelling 39, 405–410.

[4] Ardhuin Fabrice, Chapron Bertrand, Collard Fabrice (2009). Observation of swell dissipation across oceans. Geophysical Research Letters (GRL), 36(L06607), 1-5.

[5] Ardhuin, F., Rogers, E., Babanin, A., Filipot, J.-F., Magne, R., Roland, A., van der Westhuysen, A., Queffeulou, P., Lefevre, J.-M., Aouf, L., Collard, F., 2010. Semi-empirical dissipation source functions for wind-wave models: part I, definition, calibration and validation. J. Phys. Oceanogr. 40 (9), 1917–1941.

[6] Bidlot, J., Janssen, P., Abdalla, S., 2005. A revised formulation for ocean wave dissipation in CY25R1. Tech. Rep. Memorandum R60.9/JB/0516, Research Department, ECMWF, Reading, U. K.

[7] Bidlot, J., Janssen, P., Abdalla, S., 2007. A revised formulation of ocean wave dissipation and its model impact. Tech. Rep. Memorandum 509, ECMWF, Reading, U. K.

[8] Boudière, E., Maisondieu, C., Ardhuin, F., Accensi, M., Pineau-Guillou, L., Lepesqueur, J., 2013. "A suitable metocean hindcast database for the design of marine energy converters". Int. J. Mar. Energy 28 (3–4), e40–e52.

[9] Carrère, L., Lyard, F., Cancet, M., & Guillot, A. (2015, April). FES 2014, a new tidal model on the global ocean with enhanced accuracy in shallow seas and in the Arctic region. In EGU general assembly conference abstracts (p. 5481).

[10] Copernicus Marine In Situ Tac Data Management Team, 2020. Product User Manual for multiparameter Copernicus In Situ TAC (PUM). https://doi.org/10.13155/43494

[11] Dee, D. P., Uppala, S. M., Simmons, A. J., Berrisford, P., Poli, P., Kobayashi, S., Andrae, U., Balmaseda, M. A., Balsamo, G., Bauer, P., Bechtold, P., Beljaars, A. C. M., van de Berg, L., Bidlot, J., Bormann, N., Delsol, C., Dragani, R., Fuentes, M., Geer, A. J., Haimbergere, L., Healy, S. B., Hersbach, H., Holm, E. V., Isaksena, L., Køallberg, P., Kohler, M., Matricardi, M., McNally, A. P., Monge-Sanz, B. M., Morcrette, J.-J., Park, B.-K., Peubey, C., de Rosnay, P., Tavolato, C., Thepaut, J.-N., Vitart, F., 2011. The era-interim reanalysis: configuration and performance of the data assimilation system. Quart. Journ. Roy. Meteorol. Soc. 137, 553–597.

[12] Dodet, G., Piolle, J.-F., Quilfen, Y., Abdalla, S., Accensi, M., Ardhuin, F., Ash, E., Bidlot, J.-R., Gommenginger, C., Marechal, G., Passaro, M., Quartly, G., Stopa, J., Timmermans, B., Young, I., Cipollini, P., Donlon, C., 2020. The sea state cci dataset v1: towards a sea state climate data record based on satellite observations. Earth System Sciences. Data 12, 1929–1951.

[13] Gallagher, S., Tiron, R. & Dias, F. (2014) A long-term nearshore wave hindcast for Ireland: Atlantic and Irish Sea coasts (1979–2012). Ocean Dynamics 64, 1163–1180. https://doi.org/10.1007/s10236-014-0728-3

[14] Girard-Ardhuin, F., Ezraty, R., 2012. Enhanced arctic sea ice drift estimation merging radiometer and scatterometer data. IEEE Trans. on Geosci. and Remote Sensing 50, 2639–2648.

[15] Grant, W. D., and O. S. Madsen (1979), Combined wave and current interaction with a rough bottom, J. Geophys. Res., 84(C4), 1797-1808.

[16] Hasselmann, S., Hasselmann, K., Allender, J., Barnett, T., 1985. Computation and parameterizations of the nonlinear energy transfer in a gravity-wave spectrum. Part II: Parameterizations of the nonlinear energy transfer for application in wave models. J. Phys. Oceanogr. 15, 1378–1391.

[17] Hersbach, H., Bell, B., Berrisford, P., Hirahara, S., Horányi, A., Muñoz-Sabater, J., Nicolas, J., Peubey, C., Radu, R., Schepers, D., Simmons, A., Soci, C., Abdalla, S., Abellan, X., Balsamo, G., Bechtold, P., Biavati, G., Bidlot, J., Bonavita, M., Chiara, G. D., Dahlgren, P., Dee, D., Diamantakis, M., Dragani, R., Flemming, J., Forbes, R., Fuentes, M., Geer, A., Haimberger, L., Healy, S., Hogan, R. J., Hólm, E., Janisková, M., Keeley, S., Laloyaux, P., Lopez, P., Lupu, C., Radnoti, G., de Rosnay, P., Rozum, I., Vamborg, F., Villaume, S., Thépaut, J., 2020. "The ERA5 global reanalysis". Quart. Journ. Roy. Meteorol. Soc. 146, 1999–2049.

[18] Janssen, P. A. E. M., 1991. Quasi-linear theory of wind wave generation applied to wave forecasting. J. Phys. Oceanography. 21, 1631-1642, see complements by D. Chalikov, J. Phys. Oceanography. 1993, vol. 23 pp. 1597-1600.

[19] Lazure P., Dumas F., 2008. An external-internal mode coupling for a 3D hydrodynamical model for applications at regional scale (MARS). Advances In Water Resources, 31(2), 233-250. http://dx.doi.org/10.1016/j.advwatres.2007.06.010

[20] Leckler, F., 2013. Observation et modélisation du déferlement des vagues. Ph.D. thesis, Université Européenne de Bretagne, École doctorale des Sciences de la Mer, Brest, France.

[21] Leonard, B. P., 1991. The ULTIMATE conservative difference scheme applied to unsteady one-dimensional advection. Computational Methods Applied in Mechanical Engineering 88, 17-74.

[22] Perignon, Y. (2017). Assessing accuracy in the estimation of spectral content in wave energy resource on the French Atlantic test site SEMREV. Renewable Energy, 114, 145-153.

[23] Perignon, Y., & Maisondieu, C. (2017, August). Assessing accuracy of hindcast spectral content in the estimation of wave energy resource. In European Wave and Tidal Energy Conference.

[24] Pineau-Guillou, L., 2013. Validation des atlas de composantes harmoniques de hauteurs et courants de marée. (https://marc.ifremer.fr/content/download/7861/41823/file/2013_06_12_rap_valid_atlas_V1.pdf)

[25] Pineau-Guillou Lucia, Ardhuin Fabrice, Bouin Marie-Noëlle, Redelsperger Jean-Luc, Chapron Bertrand, Bidlot Jean-Raymond, Quilfen Yves (2018). Strong winds in a coupled wave-atmosphere model during a North Atlantic storm event: evaluation against observations. Quarterly Journal Of The Royal Meteorological Society, 144(711 Part.B), 317-332.

[26] Roland, A., Development of WWM II: Spectral Wave Modelling on Unstructured Meshes, Ph. D. thesis, Inst. of Hydraul. and Wave Resour. Eng., Darmstadt University of Technology, Germany, 2008.

[27] Roland, A. Cucco, A., Ferrarin, C., Hsu, T.-W., Liau, J.-M., Ou, S.-H., Umgiesser, G., Zanke, U., On the development and verification of 2-D coupled wave-current model on unstructured meshes, J. Mar. Syst. 78 (2009) S244–S254.

[28] Roland Aron, Ardhuin Fabrice (2014). On the developments of spectral wave models: numerics and parameterizations for the coastal ocean. Ocean Dynamics, 64(6), 833-846.

[29] The European Marine Energy Centre (2020). BC-DWR-E-2017, EMEC Datawell Waverider data at full scale wave test site at Billia Croo, Orkney, UK. SEANOE. https://doi.org/10.17882/77343

[30] Stopa, J. E., Ardhuin, F., Stutzmann, E., Lecocq, T., 2019. Sea state trends and variability: consistency between models, altimeters, buoys, and seismic data (1979-2016). J. Geophys. Res. 124, in press.

[31] The WAVEWATCH III ® Development Group, 2019. User manual and system documentation of WAVEWATCH III ® version 6.07. Tech. Note 333, NOAA/NWS/NCEP/MMAB, College Park, MD, USA, 465 pp. + Appendices.

[32] Tournadre, J., Bouhier, N., Girard-Ardhuin, F., Remy, F., 2016. Antarctic iceberg distributions 2002–2010. J. Geophys. Res. 121, 327–349.

[33] Cerema. Fiches synthétiques de mesure des états de mer - Tome 1 – Mer du Nord, Manche et Atlantique - Janvier 2021Cerema, 2021. Collection : Données. ISBN : 978-2-37180-497-